α-Monoacylated and α,α′- and α,β′-Diacylated Dipyrrins as Highly Sensitive Fluorescence "Turn-on" Zn2+ Probes

ARTICLE *in* THE JOURNAL OF ORGANIC CHEMISTRY · MAY 2013

Impact Factor: 4.72 · DOI: 10.1021/jo400454e · Source: PubMed

JOC The Journal of Organic Chemistry

Article

pubs.acs.org/joc

α-Monoacylated and α,α′- and α,β′-Diacylated Dipyrrins as Highly Sensitive Fluorescence "Turn-on" Zn^{2+} Probes

Yubin Ding,[†] Xin Li,[‡] Tong Li,[†] Weihong Zhu,[†] and Yongshu Xie*,[†]

[†]Key Laboratory for Advanced Materials and Institute of Fine Chemicals, East China University of Science and Technology, Shanghai 200237, People's Republic of China

[‡]Department of Theoretical Chemistry and Biology, School of Biotechnology, KTH Royal Institute of Technology, SE-10691 Stockholm, Sweden

Supporting Information

ABSTRACT: With the purpose of developing readily synthesized CHEF (chelation-enhanced fluorescence) type Zn^{2+} probes with relatively simple molecular structures and excellent sensing behavior, *p*-anisoyl chloride was used for the acylation of 5-(pentafluorophenyl)dipyrromethane. Interestingly, the α,β′-diacylated product **PS2** with a unique substitution mode was obtained in high yield in addition to the normal α-substituted mono- and diacylated products **PS1** and **PS3**. Further oxidation of **PS1**−**PS3** afforded dipyrrins **S1**−**S3**. Crystal structure and ^{1}H NMR measurements of **S2** demonstrate the existence of a pure tautomer, which is consistent with DFT calculations. **S1**−**S3** show highly Zn^{2+} selective "turn-on" fluorescence based on a CHEF mechanism by the formation of 2:1 (probe:metal) Zn^{2+} complexes. The emission colors can be easily tuned from green to red by changing the dipyrrin substitution modes. Furthermore, these probes demonstrate fast responses and wide applicable pH ranges. Among them, **S2** shows the highest Zn^{2+} sensitivity, with a detection limit of 4.4×10^{-8} M.

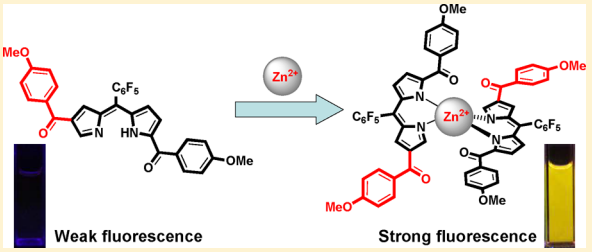

INTRODUCTION

Synthetic fluorescent ion probes are highly valuable tools for the selective recognition of chemically and biologically important ions, with the advantages of convenient utilization, high sensitivity, rapid response, and low cost.[1] Zinc ion plays vital roles in numerous biological processes.[2] Thus, Zn^{2+} sensing based on fluorescence quenching or enhancement has attracted increasing interest in recent years.[1i,3] Fluorescence quenching may be caused by a number of factors other than the target analyte, and thus the sensing behavior may be nonspecific. Thus, "turn-on" type fluorescent Zn^{2+} probes are highly desirable. For the development of such probes, usually a binding moiety is linked by a bridge to a fluorophore, which acts as the reporting moiety. Representative fluorophores include fluorescein,[4] anthracene,[5] naphthalimide,[6] coumarin,[7] quinoline,[8] cyanine dyes,[9] rhodamine,[10] and BODIPY.[11] With use of these fluorophores, a number of "turn-on" type fluorescent Zn^{2+} probes have been developed on the basis of various sensing mechanisms, including PET (photoinduced electron transfer),[12] ICT (intramolecular charge transfer),[13] FRET (fluorescence resonance energy transfer),[14] excimer,[15] AIE (aggregation induced emission),[16] and CHEF (chelation-enhanced fluorescence).[17] Among these, CHEF type probes are based on the simple idea that intramolecular rotations will be suppressed by chelation so that nonradiative energy loss of the excited state will be decreased and thus the fluorescence will be enhanced. For the design of such probes, there is no need to modulate complicated electron or charge transfer processes or complicated intermolecular interactions, and the binding moiety may simultaneously act as the reporting moiety. Thus, the molecular structure may be relatively simple and easy to design and synthesize.[18] In addition, chelation effects usually induce strong binding, and the resulting probes may have high sensitivity. However, it is still a challenging task to develop easily synthesized CHEF type Zn^{2+} probes with novel structures and a combination of excellent sensing behavior including fast response, low detection limit, and wide applicable pH range.

As a component of BODIPY, dipyrrins consist of two pyrrolic units connected by an sp^2 meso carbon atom, and the conjugated π system gives rise to an intense absorption in visible region.[19] In recent years, dipyrrins have been used as bidentate monoanionic ligands for various applications such as the construction of interesting supermolecular structures and syntheses of fluorescent metal complexes.[19b,20] In this respect, Cheprakov and co-workers synthesized π-extended dipyrrins capable of forming brightly fluorescent Zn^{2+} complexes.[21] In addition, boron complexes of dipyrrins (BODIPY) are well-known for their excellent fluorescence properties.[22] Encouraged by this inspiring research on highly fluorescent dipyrrin complexes and the fact that dipyrrin itself has rather weak fluorescence, we reported dipyrrins **D1**−**D3** as "turn on" type fluorescent Zn^{2+} probes based on a CHEF mechanism[23] and

Received: March 8, 2013
Published: May 13, 2013

demonstrated that the substituents at the α positions of the pyrrolic units greatly affect the sensing behavior.

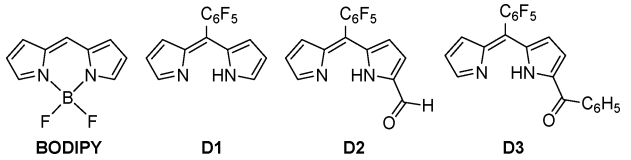

On the basis of our previous work on the aforementioned Zn^{2+} probes and other relevant systems in this area,[23,24] we envisioned that further introduction of electron-donating groups to the benzoyl substituent of the **D3** molecule may further enhance its coordination with Zn^{2+} and thus further improve the Zn^{2+} detection sensitivity. Therefore, we attempted to acylate 5-(pentafluorophenyl)dipyrromethane by Friedel–Crafts reactions, using *p*-anisoyl chloride as an acylating agent. It is well-known that the acylation of dipyrromethanes with pentafluorobenzoyl chloride and some other acid chlorides always afford α-monoacylated and α,α'-diacylated dipyrromethanes, which have been widely used for the syntheses of porphyrins and porphyrinoids.[25] In contrast to this, we unexpectedly obtained the α,β'-diacylated product **PS2** in a yield of 48% accompanied by the normal α-substituted mono- and diacylated products **PS1** and **PS3** (Figure 1a). Oxidation of **PS1**–**PS3** with DDQ (2,3-dichloro-5,6-dicyano-1,4-benzoquinone) afforded acylated dipyrrins **S1**–**S3**, which show a CHEF type "turn on" fluorescence upon addition of Zn^{2+}. The detection limit of **S2** for Zn^{2+} was calculated to be 4.4×10^{-8} M, which is more sensitive than the normal α-substituted mono- and diacylated products **S1** and **S3**.

The control and tuning of emission wavelengths and colors of fluorescent probes can expand their multiplexing capability in practical applications, thus drawing much attention from the scientific community.[26] In this work, by changing the numbers and positions of the substituents, the calculated HOMO–LUMO energy gaps of Zn^{2+} complexes of **S1**–**S3** decreased successively, resulting in a concomitant successive increase of the emission maxima wavelengths, with the emission colors varying from green to red. Furthermore, competition experiments demonstrated that **S1**–**S3** can selectively detect Zn^{2+} in both DMF- and water-containing systems. Thus, probes **S1**–**S3** can be developed as a novel and promising type of highly sensitive and selective "turn-on" fluorescent Zn^{2+} probes with tunable emission colors. Impressively, **S2** shows a unique α,β'-substitution mode, good sensitivity, and orange emission color.

RESULTS AND DISCUSSION

Syntheses and Characterization of Probes S1–S3. Compounds **S1**–**S3** were readily synthesized by acylation of 5-(pentafluorophenyl)dipyrromethane with *p*-anisoyl chloride, followed by oxidation with DDQ, and fully characterized by ^{1}H NMR, ^{13}C NMR, and HRMS (Figure 1a and Figures S1–S18 (Supporting Information)). As we know, acylated dipyrromethanes are important intermediates for the syntheses of porphyrins and porphyrinoids, because they can be easily reduced to the corresponding alcohols and then used for further condensation with pyrrolic derivatives.[25a,b] Especially, pentafluorobenzoyl-substituted dipyrromethanes have attracted extensive interest in this area due to the fact that most expanded porphyrins with *meso*-pentafluorophenyl groups have better stability than those with other aryl substituents.[27] It is well-known that electrophilic acylation reaction of pyrrole occurs at an α-carbon atom, the position adjacent to the nitrogen atom, because attack of an electrophile at the α-position leads to a more stable cationic intermediate with three resonance forms, while reaction at a β-carbon atom gives a less stable cation with only two resonance forms.[28] Thus, the typical acylation of a dipyrromethane through the Friedel–Crafts reaction will afford two products: namely, the α-monoacyl dipyrromethane and the α,α'-diacyl dipyrromethane.[29] In this work, with the aim of increasing the Zn^{2+} binding ability of the resulting dipyrrins, we used *p*-anisoyl chloride to acylate the dipyrromethane by a Friedel–Crafts reaction. Unexpectedly, three main products were observed by TLC analysis. After separation of the crude product by silica gel columns, we obtained products **PS1**–**PS3**. ^{1}H NMR measurements revealed that **PS1** is an α-monoacyl product with two types of pyrrolic NH signals (Figure 1b). The ^{1}H NMR of **PS3** demonstrated a symmetrical structure with only one type of pyrrolic NH, which is consistent with an α,α'-diacyl structure (Figure 1b). The ^{1}H NMR of **PS2** shows the same hydrogen number as **PS3**, but the hydrogen signals are rather unsymmetrical, exhibiting two types of pyrrolic NH signals (Figure 1b), indicating that **PS2** is also a diacyl product but the substitution mode is different from that of **PS3**. HRMS of **PS2** and **PS3** also shows almost identical molecular peaks at 581.1498 and 581.1497 ($[M + H]^+$, Figures S6 and S9 (Supporting Information)), which further indicates that **PS2** should be a diacyl product and that one of the acyl substituents must not be attached to the α position. To clearly elucidate the identity of the structure of **PS2**, the ^{1}H–^{1}H COSY NMR spectrum (Figure 2) of **PS2** was collected. It can

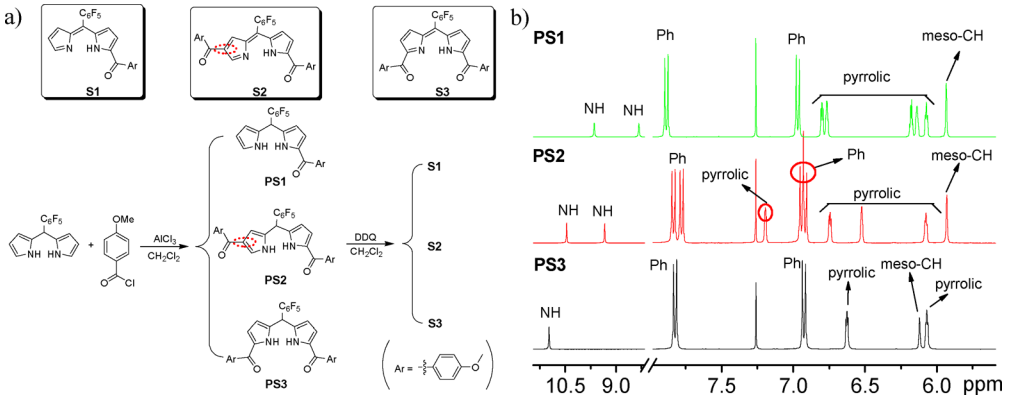

Figure 1. (a) Syntheses and structures of probes **S1**–**S3**. (b) Low-field region of the ^{1}H NMR spectra of **PS1**–**PS3** ($CDCl_3$, 400 MHz, 298 K).

dx.doi.org/10.1021/jo400454e | J. Org. Chem. 2013, 78, 5328–5338

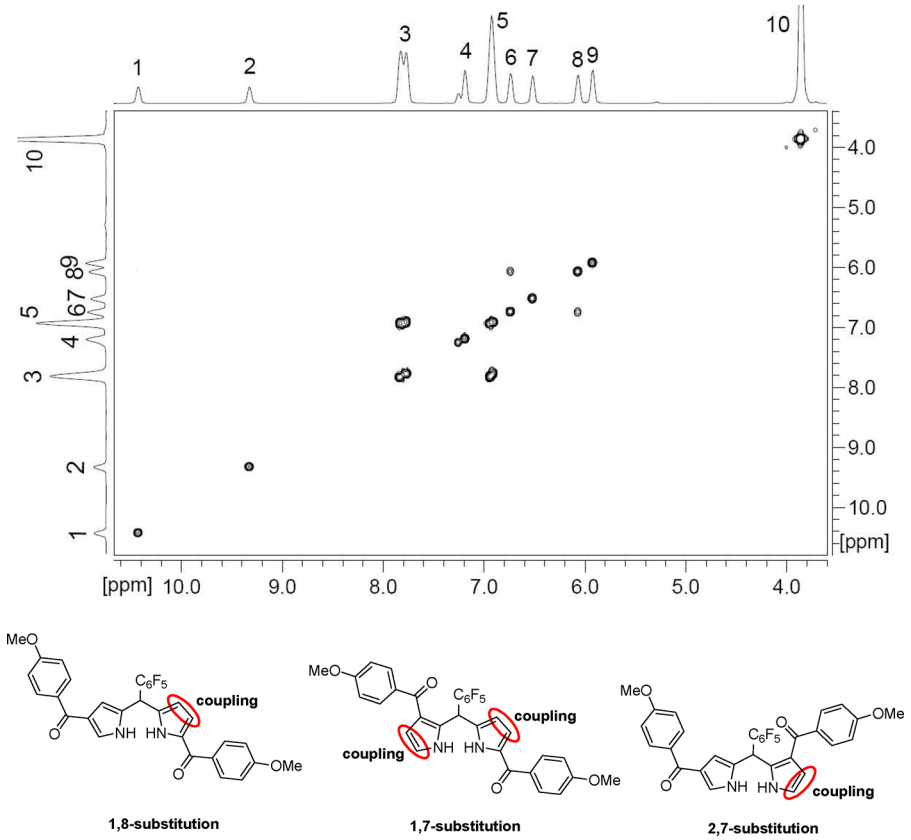

Figure 2. ^{1}H−^{1}H COSY NMR spectrum of **PS2** (500 MHz in $CDCl_3$ at 298 K) with the coupling modes between the pyrrolic hydrogens shown for all possible unsymmetric isomers.

be observed that the hydrogens at ∼7.8 ppm (peak 3) couple with those at ∼6.9 ppm (peak 5) and the hydrogen at ∼6.75 ppm (peak 6) couples with that at ∼6.08 ppm (peak 8). Considering the coupling modes, chemical shifts, and hydrogen numbers, the peaks at ∼7.8 and ∼6.9 ppm can be assigned to the eight phenylene hydrogens, and the peaks at ∼6.75 and ∼6.08 ppm can be assigned to two pyrrolic hydrogens, with two uncoupled pyrrolic hydrogens left at ∼7.2 ppm (peak 4) and ∼6.5 ppm (peak 7), respectively. Only the 1,8- or the 2,7-substituted structure (Figure 2) is consistent with these observations. On the other hand, the α-pyrrolic hydrogens usually appear at lower field than the β hydrogens, and in the ^{1}H NMR spectrum of **PS2**, only one typical α-hydrogen can be observed at ∼7.2 ppm, which is consistent with the 1,8-substitution mode. This assignment is also in agreement with the crystal structure of the corresponding oxidized product (vide infra). The mechanism for the generation of the α,β'-diacylated product is still unclear to us at the present stage. It is well-known that the utilization of pentafluorobenzoyl chloride as the acylating agent always affords the α- and α,α'-substituted products.[27b] Thus, the generation of the α,β'-diacylated product may be related to the electron-donating effect of the methoxy substituent on the benzoyl chloride.

We then tried to oxidize **PS1**−**PS3** by DDQ in CH_2Cl_2. **PS1** was easily oxidized to compound **S1** by stirring with 2.0 equiv of DDQ for 1 h in a yield of 61%. **PS2** and **PS3** were more difficult to oxidize. More DDQ and/or longer times were required. Thus, **PS2** was successfully oxidized to compound **S2** by 2.0 equiv of DDQ for 24 h in a yield of 69%, and 8 equiv of DDQ and a longer time of 36 h were required for the oxidation of **PS3** to **S3** in a high yield of 97%. To further elucidate the substitution mode of **PS2** and the corresponding oxidized product **S2**, we tried to grow their single crystals. Fortunately, single crystals of **S2** were obtained and analyzed by X-ray diffraction, which clearly indicated that the *p*-anisoyl groups were really attached to the α,β'-positions of the pyrrolic units (Figure 3a), as expected from the aforementioned results. To the best of our knowledge, this is the first example of an α,β'-diacylated dipyrrin utilized for Zn^{2+} detection.

Theoretically, unsymmetrically substituted dipyrrins have two tautomeric forms (Scheme 1), with the proton shifting very fast between the two pyrrolic units. Interestingly, both crystal structure and ^{1}H NMR measurements clearly demonstrate that **S2** exists in a pure tautomeric form whose proton is bound to the α-acylated pyrrolic nitrogen (Figure 3a and Figure S13 in the Supporting Information). In the crystal structure, the C4−C5 and C5−C6 bond lengths are observed to be 1.440(3) and 1.367(3) Å, respectively. These values are typical of C−C single bonds and C=C double bonds, respectively. The C1−N1−C4 bond angle has a large value of 110.8(2)°, which is typical for a pyrrolic amino NH moiety. Also, the C9−N2−C6 bond angle has a much smaller value of 105.2(2)°, which is in agreement with a typical pyrrolic imino N moiety. It is noteworthy that the imino N2 atom is involved in an intramolecular hydrogen bond with the amino NH donor, with an H1···N2 distance of 2.09 Å. In addition, two classes of intermolecular hydrogen bonds are observed between the phenyl hydrogen atoms and the oxygen atoms from the methoxy and the carbonyl moieties, with O···H distances of 2.48 and 2.43 Å, respectively. The corresponding C−H···O angles are 154 and 164°, respectively. Finally, a 2D supramolecular network is formed by linkage of the intermolecular hydrogen bonds (Figure 3b). The wide

dx.doi.org/10.1021/jo400454e | J. Org. Chem. 2013, 78, 5328−5338

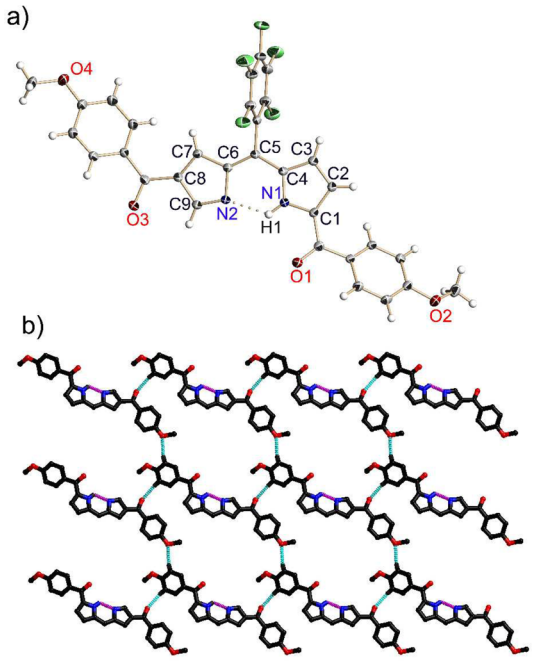

Figure 3. (a) Crystal structure of compound **S2** with ellipsoids shown at the 20% probability level. (b) 2D supramolecular network formed by the linkage of intra- and intermolecular hydrogen bonds. The pentafluorophenyl groups and non-hydrogen-bonded H atoms are omitted for clarity.

Scheme 1. Interconversion between Two Tautomeric Forms of S2

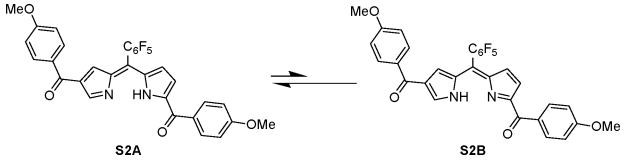

occurrence of intra- and intermolecular hydrogen bonds may be favorable for the stabilization of the clearly fixed tautomer and conformation. These results are in agreement with DFT calculations, which reveal that the free energy of the tautomeric form **S2A** is 13.2 kJ mol^{-1} lower than that of **S2B** (Scheme 1), resulting in a **S2A**:**S2B** ratio of 1:0.005. Similarly, compound **S1** also predominantly exists in such a tautomeric form whose proton is bound to the α-acylated pyrrolic nitrogen, and the free energy of **S1A** is 10.3 kJ mol^{-1} lower than that of **S1B**, resulting in a **S1A**:**S1B** ratio of 1:0.016 (Figures S19 and S20 in the Supporting Information).[30]

Titration Study. Compounds **S1**−**S3** show rather weak fluorescence in DMF, with small quantum yield values of 0.013, 0.017, and 0.005, respectively, using rhodamine 6G as a reference.[31] Upon addition of Zn^{2+} to respective solutions of probes **S1**−**S3**, significant fluorescence enhancement was apparent to the naked eye. To investigate the Zn^{2+} sensing behavior in detail, UV−vis and fluorescence spectral changes of these probes upon gradual addition of Zn^{2+} were measured in both DMF and aqueous solutions (DMF/50 mM HEPES, 4/1 v/v, pH 7.4). For **S2**, for example, the titration of Zn^{2+} to its DMF solution induced a hypsochromic shift from 550 to 544 nm (Figure 4a). A set of isosbestic points was observed at 300, 386, 485, and 558 nm, indicating the formation of a well-defined complex between **S2** and Zn^{2+}. This process was accompanied by a sharp fluorescence "turn-on" behavior. As shown in Figure 4b, the solution of **S2** showed very weak fluorescence before the addition of Zn^{2+}. When Zn^{2+} was gradually added, its fluorescence intensity was significantly enhanced, with the emission peak centered at about 571 nm. Similar spectral changes were observed when the solutions of **S1** and **S3** were titrated with Zn^{2+} (Figures S21a and S22a in the Supporting Information). Vivid fluorescence enhancement was observed with the emission peaks centered at 549 and 588 nm for **S1** and **S3**, respectively (Figures S21b and S22b in the Supporting Information). These results are indicative of good fluorescence "turn-on" type Zn^{2+} detection capability of compounds **S1**−**S3**. Hence, we continued to check the sensing mechanism in detail.

Sensing Mechanism. Before addition of Zn^{2+}, the free probes **S1**−**S3** show very weak background fluorescence. This can be ascribed to a loss of excited state energy via free rotation of pyrrolic units in the molecules. From the aforementioned titration results, we found that addition of 0.5 equiv of Zn^{2+} to solutions of **S2** almost saturated its UV−vis and fluorescence spectral changes, suggesting that **S2** forms a 2:1 complex with Zn^{2+}. This conclusion is consistent with the corresponding Job plot, wherein the fluorescence intensity reaches a peak when the ratio **S2**:Zn^{2+} is 2:1 (Figure S23 in the Supporting Information). The 2:1 binding stoichiometry was also observed in the Job plots for **S1** and **S3** (Figures S24 and S25 in the Supporting Information). These results indicate that the fluorescence enhancement is induced by the formation of 2:1 Zn^{2+} complexes of probes **S1**−**S3**. From nonlinear fitting of the

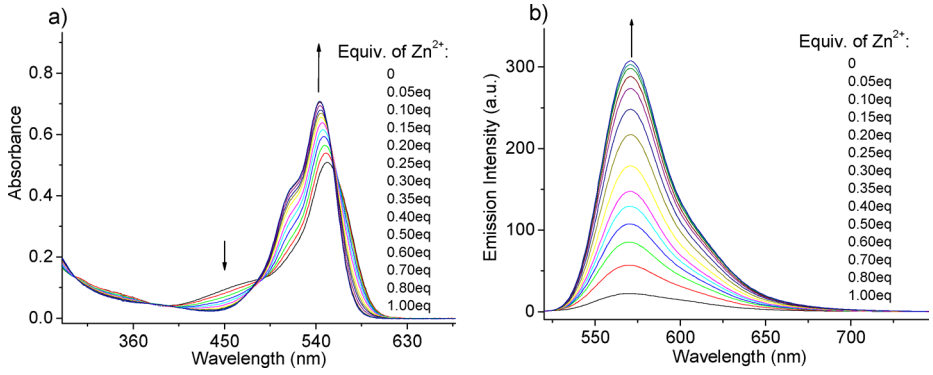

Figure 4. (a) UV−vis spectral changes during a titration of **S2** (10 μM) with Zn^{2+} in DMF. (b) Corresponding fluorescence emission spectral changes with λ_{ex} fixed at 485 nm (one of the isosbestic points).

dx.doi.org/10.1021/jo400454e | J. Org. Chem. 2013, 78, 5328−5338

fluorescence data according to a 2:1 binding model,[32] Zn^{2+} binding constants were calculated to be 5.0×10^{13}, 2.2×10^{13}, and 2.1×10^{13} M^{-2} for **S1**–**S3**, respectively (Figures S26–S28 in the Supporting Information). To further elucidate the coordination structure, we successfully synthesized complexes $Zn(\mathbf{S1})_2$, $Zn(\mathbf{S2})_2$, and $Zn(\mathbf{S3})_2$ in high yields by stirring **S1**–**S3** with $Zn(OAc)_2{\cdot}2H_2O$ in MeOH, and the complexes were fully characterized by ^1H NMR, ^{13}C NMR, HRMS, and IR (Figures S29–S37 in the Supporting Information). In comparison to free probes **S1**–**S3**, ^1H NMR signals of $Zn(\mathbf{S1})_2$–$Zn(\mathbf{S3})_2$ were clearly shifted upfield, and in the HRMS, molecular peaks were observed at 951.1003, 1219.1744, and 1219.1747 ($[M + H]^+$), respectively. These values are in accordance with the calculated values. Fortunately, single crystals of $Zn(\mathbf{S1})_2$ were obtained by slow evaporation of a $MeOH/H_2O$ solution of $Zn(\mathbf{S1})_2$. X-ray diffraction analyses clearly revealed a 2:1 coordination mode, which is consistent with the aforementioned results. The carbonyl O atoms are weakly coordinated to Zn^{2+}, with Zn–O1 and Zn–O3 bond lengths of 2.37(9) and 2.46(2) Å, respectively. These values are similar to those observed for our previously reported dipyrrin zinc complexes.[23] In the molecule of $Zn(\mathbf{S1})_2$, the coordinated dipyrrin is nearly planar, showing a rather small dihedral angle of 6.8° between the two pyrrolic units (Figure 5).

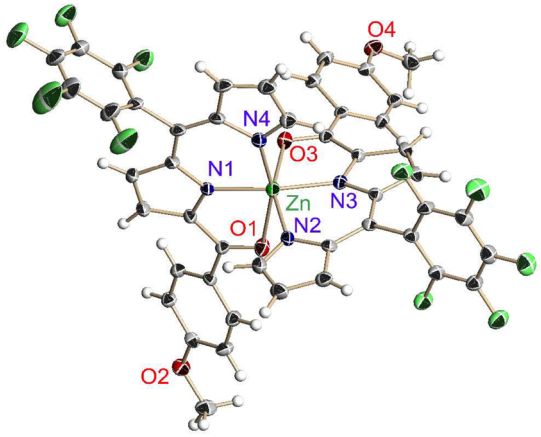

Figure 5. X-ray crystal structure of $Zn(\mathbf{S1})_2{\cdot}MeOH$ complex with ellipsoids shown at the 20% probability level. The methanol solvent is omitted for clarity.

Thus, addition of Zn^{2+} to solutions of **S1**–**S3** leads to the formation of the corresponding zinc complexes with a 2:1 stoichiometry, and the resulting complexes are more rigid and planar than corresponding free probes and loss of excited-state energy through intramolecular rotations is suppressed, which results in the observed chelation-enhanced fluorescence (CHEF).[23]

Emission Color Modulation. Ready control and modulation of emission wavelengths of fluorescent probes are critically important for expanding their multiplexing capability of various application requirements.[26] As shown in Figure 6, upon addition of 1 equiv of Zn^{2+}, solutions of probes **S1**–**S3** show emission colors varying from green to red. These differences originate from the difference in the size of π-electron conjugation systems caused by the substituents in the molecules. Only one *p*-anisoyl substituent is attached to one of the pyrrolic units of probe **S1**, which results in the smallest π-electron conjugation system, while **S2** has one additional *p*-anisoyl group at the β-position of the other pyrrolic unit, which enlarges the π-electron conjugation system. In **S3**, two *p*-anisoyl substituents were also introduced, with both of them attached to the α-positions of the pyrrolic units, which results in conjugation even better than that of **S2**. Thus, red shifting of the emission colors from **S1** to **S3** can be rationalized by the increasing size of π-electron conjugation systems. To gain further insight, we performed density functional calculations on optimized geometries of the complexes employing the hybrid B3LYP function. The HOMO–LUMO energy gaps of $Zn(\mathbf{S1})_2$, $Zn(\mathbf{S2})_2$ and $Zn(\mathbf{S3})_2$ were calculated to be 2.89, 2.78, and 2.67 eV, respectively. These results indicate that the decrease of HOMO–LUMO energy gaps results in a concomitant successive increase of the emission maxima wavelengths (Figure 7). Thus, it can be concluded that tuning of the emission colors of the dipyrrins can be conveniently realized by changing the substituent numbers and positions. These results demonstrate that probes **S1**–**S3** provide good examples of a convenient designing strategy for novel emission color tunable fluorescent probes or light-emitting organic materials.

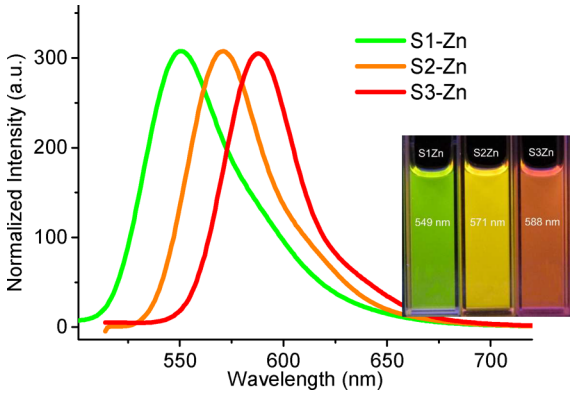

Figure 6. Fluorescence spectra of probes **S1**–**S3** (10 μM) in the presence of 1 equiv of Zn^{2+} in DMF. The inset shows corresponding photographs under 365 nm UV light.

High Sensitivity. The detection limit is one of the most important parameters in cation sensing. For many practical purposes, it is very important to detect the analytes at low concentrations. The detection limits of probes **S1**–**S3** for Zn^{2+} were obtained according to the reported method.[33] We take **S2** as an example: first a titration of **S2** (0.1 μM) with Zn^{2+} (0–0.12 μM) was carried out in DMF, and fluorescence changes during the titration were recorded and are shown in Figure S38a (Supporting Information). The enhancement of fluorescence intensity during gradual addition of Zn^{2+} was clearly observed with a good signal-to-noise ratio. Then a plot of $(I - I_{min})/(I_{max} - I_{min})$ versus log $[Zn^{2+}]$ was drawn (Figure S38a, inset, in the Supporting Information), where I_{max} represents the maximum fluorescence intensity observed upon the addition of 0.12 μM Zn^{2+} and I_{min} represents the minimum fluorescence intensity of probe **S2** before the addition of Zn^{2+}. Thus, a good linear relationship could be obtained in the range 10 nM–0.1 μM. A linear regression of the five intermediate values (Figure S38b in the Supporting Information) afforded an intercept of −7.36 at the *x* axis, which corresponds to the detection limit of 4.4×10^{-8} M. Similarly, detection limits of **S1** and **S3** were found to be 2.6×10^{-7} and 1.7×10^{-7} M, respectively (Figures S39 and S40 in the Supporting Information). These data indicate that all three probes show high sensitivity toward Zn^{2+}.

dx.doi.org/10.1021/jo400454e | J. Org. Chem. 2013, 78, 5328–5338

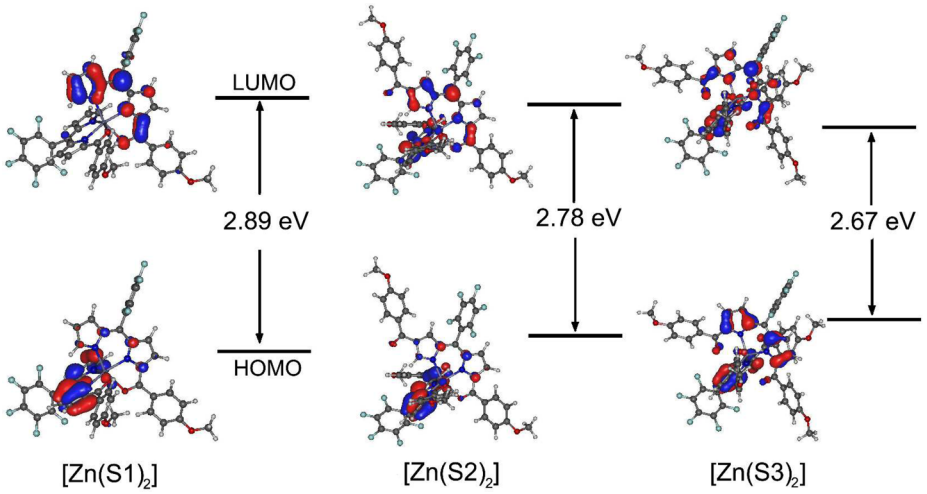

Figure 7. Frontier orbital energy diagrams of $[Zn(\mathbf{S1})_2]$, $[Zn(\mathbf{S2})_2]$, and $[Zn(\mathbf{S3})_2]$.

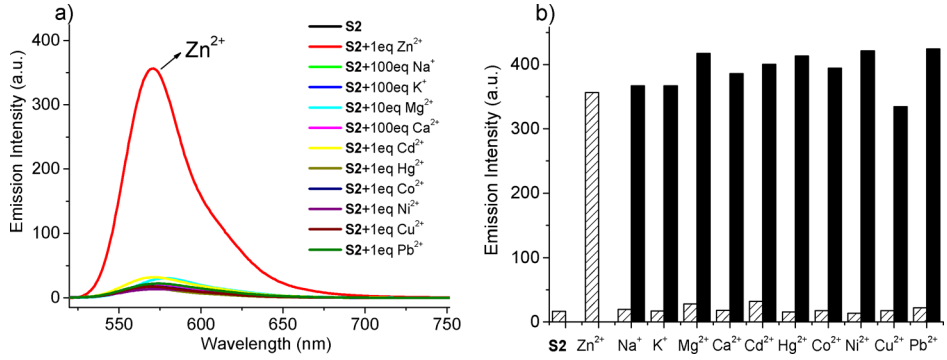

Figure 8. Relative fluorescence intensity of 10 μM **S2** in DMF upon excitation at 485 nm (one of the isosbestic points): (a) spectra in the presence of various metal ions; (b) graph with white bars representing the addition of 1 equiv of metal ions (100 equiv for Na^+, K^+, and Ca^{2+} and 10 equiv for Mg^{2+}) and black bars representing the addition of 1 equiv of Zn^{2+} mixed with 1 equiv of the indicated metal ions (100 equiv for Na^+, K^+, and Ca^{2+} and 10 equiv for Mg^{2+}).

The detection limits at the 10^{-7} M level for **S1** and **S3** are comparable to those for our previously reported dipyrrin-based Zn^{2+} probes **D1**−**D3**.[23] It can be concluded that the number of α-substituted acyl groups does not significantly affect the sensitivity of the probes. It is noteworthy that **S2** shows the lowest detection limit of 4.4×10^{-8} M, indicating that the α,β'-diacylation mode affords the best sensitivity toward Zn^{2+}. Thus, **S2** can be applied to detect Zn^{2+} at an extremely low concentration level of 10^{-8} M, which may fully meet the requirements in biosensing, as labile Zn^{2+} in the human body was reported to exist at a millimolar concentration level.[34] The higher sensitivity of probe **S2** in comparison with **S1** and **S3** may be rationalized by the following observations. Upon addition of 1 equiv of Zn^{2+} to the respective solutions of probes **S1**−**S3**, a 33-fold fluorescence enhancement was observed for **S2**, while only 10-fold and 9-fold enhancements were observed for **S1** and **S3**, respectively. Therefore, to induce detectable fluorescence changes, a smaller quantity of Zn^{2+} is required for the solution of **S2**, in comparison with those of **S1** and **S3**. In other words, probe **S2** demonstrates the highest sensitivity. From these results, it can be concluded that the substitution position has a great influence on the sensing sensitivity.

Zn^{2+} Selectivity. In addition to sensitivity, selectivity is another major issue in the field of ion sensing. For an ideal fluorescent ion probe, only the target ion can induce drastic fluorescence changes, and the coexistence of other competing ions should not disturb the detection of the target ion. To our delight, probes **S1**−**S3** meet these two requirements for selective detection of Zn^{2+}. In the case of **S2** in DMF (Figure 8) or in a HEPES buffer (Figure S41 in the Supporting Information), when 1 equiv of various cations was added, only Zn^{2+} significantly enhanced the fluorescence by about 33-fold, whereas other divalent metals (Cd^{2+}, Hg^{2+}, Co^{2+}, Ni^{2+}, Cu^{2+}, Pb^{2+}, Mg^{2+}) and in vivo abundant alkali-metal cations (for Na^+, K^+, and Ca^{2+}, 100 equiv was added, since they are abundant in living systems) only induced slight fluorescence changes (Figure 8a). As is well-known, fluorescent Zn^{2+} probes may encounter interference by other cations, especially Cd^{2+} and Cu^{2+}. Thus, competition behavior was checked to further elucidate whether the coexistence of competing metal cations interferes with the detection of Zn^{2+}. In the solutions of probe **S2**, upon addition of Zn^{2+} together with other competing cations (Figure 8b and Figure S38d in the Supporting Information), similar fluorescence enhancement was clearly observed. Only the presence of Cu^{2+} slightly quenched the fluorescence. Fortunately, Cu^{2+} is not typically present at high concentrations in biochemical systems, and the interference of Cu^{2+} in potential biochemical applications of **S2** can be neglected.[35] Thus, it can be concluded that the detection of Zn^{2+} with **S2** is not seriously affected by the presence of competing metal cations. Similar measurements for **S1** and **S3** also showed that these probes have good selectivity toward

dx.doi.org/10.1021/jo400454e | J. Org. Chem. 2013, 78, 5328−5338

Zn^{2+} (Figures S42 and S43 in the Supporting Information). Accordingly, **S1**−**S3** can be established as highly sensitive and selective "turn-on" fluorescent Zn^{2+} probes.

Response Time and pH Influences. Response time is also an important practical parameter for fluorescent probes. After addition of 1 equiv of Zn^{2+} to the respective solutions of the probes, fluorescence changes were tracked as a function of time (Figure 9), which indicated that, for **S1** and **S2**, the

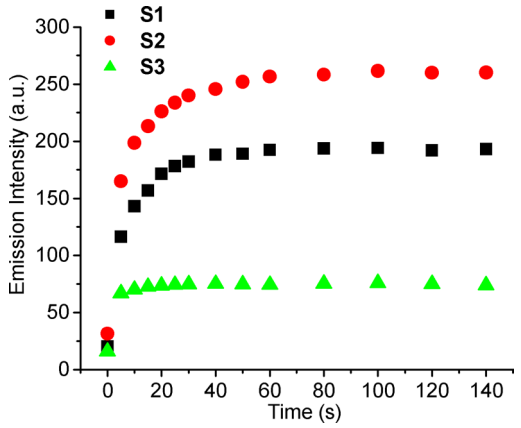

Figure 9. Time course of the fluorescence response of **S1**−**S3** (10 μM) upon addition of 1 equiv of Zn^{2+} in DMF.

fluorescence intensity reached 90% of the saturation value within 25 s. In addition, only 5 s was required for **S3** to reach 90% of the saturation fluorescence. This response time is shorter than those for most reported fluorescent probes.[7a,36] In addition to fast response, the applicable pH range is also important for practical applications. In the case of biochemical systems, it is important for the probes to work well in the neutral pH range. Thus, the influence of pH on the fluorescence of **S1**−**S3** was checked in DMF/water (4/1) solutions. The weak emission bands of **S1**−**S3** remained unaffected with increasing acidity from pH 12 to 5.0 (Figure 10 and Figures S44 and S45 in the Supporting Information). Upon addition of 1 equiv of Zn^{2+}, **S1** and **S2** exhibited drastic fluorescence enhancement, with the intensity only slightly affected by the pH value in the pH range 6.5−9.0, indicating that **S1** and **S2** work well over this wide pH range. Also for **S3**, 7.0−9.0 is a suitable pH range (Figure S45 in the Supporting

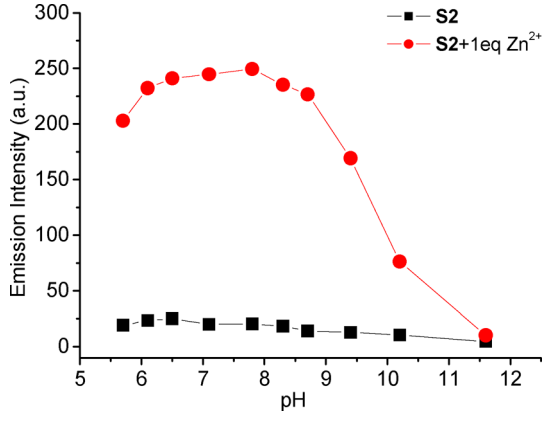

Figure 10. Relative fluorescence emission intensity of **S2** (10 μM, black squares) and **S2** + 1 equiv of Zn^{2+} (red circles) over the pH range 5−12 in DMF/water (4/1) solutions.

Information). At lower or higher pH values, fluorescence of the Zn^{2+}-containing solutions is sharply decreased, which may be attributed to the decomposition of the Zn^{2+} complexes. Under strongly acidic conditions, deprotonation of the probe molecule will be suppressed, and thus it tends to exist in the neutral and noncoordinated form. On the other hand, under strongly basic conditions, some basic species such as OH^- will displace the coordinated probe molecules from the complexes and thus decompose the fluorescent Zn^{2+} complexes, which will inactivate the probes. Therefore, the probes work effectively around the neutral pH range, which may fully meet the requirements for practical applications, such as fluorescent imaging in living cells.

CONCLUSIONS

In conclusion, with the purpose of developing readily synthesized CHEF type Zn^{2+} probes with relatively simple molecular structures and excellent sensing behavior, the three mono- and diacylated dipyrrins **S1**−**S3** were readily synthesized and developed as highly sensitive fluorescent Zn^{2+} probes. Among these compounds, **S2** shows a unique α,β'-diacylation mode. In addition, its crystal structure demonstrates the existence of a pure tautomer. Addition of Zn^{2+} to solutions of **S1**−**S3** induced drastic fluorescence enhancement, whereas other divalent or in vivo abundant alkali-metal cations only induced slight fluorescence changes. Competition experiments further demonstrated that **S1**−**S3** can selectively detect Zn^{2+} with little disturbance from other metal ions. A combination of ^{1}H NMR, HRMS, Job plots, and X-ray crystal structure analyses indicated that the fluorescence enhancement is induced by the formation of 2:1 Zn^{2+} complexes of **S1**−**S3**. These complexes have better planarity and rigidity than the corresponding probe molecules, and thus intramolecular rotation is suppressed, resulting in the "CHEF" type fluorescence enhancement. DFT calculations indicated that, from **S1** to **S3**, the HOMO−LUMO energy gaps of the corresponding Zn^{2+} complexes are decreased successively, resulting in a concomitant successive increase of the emission maxima wavelengths. Thus, the emission colors can be easily tuned from green to red by changing the substitution numbers and positions. In addition, these probes demonstrated fast response toward Zn^{2+}, and they work effectively around the neutral pH range.

In summary, novel acylated dipyrrins were synthesized and applied as fluorescence "turn-on" Zn^{2+} probes with the advantages of high sensitivity, high selectivity, fast response, wide applicable pH range, and tunable emission colors. In comparison with most porphyrin-based zinc probes,[37] the dipyrrin-derived probes have the advantages of easy synthesis and modification, and they demonstrated higher sensitivity and faster response to Zn^{2+}, because porphyrins have rigid macrocyclic structures, which results in relatively slow coordination reactions and weak CHEF effects due to the negligible rigidity enhancement upon coordination. The detection limit of **S2** reached a low value at the 10^{-8} M level, which is comparable to the limits reported for the best fluorescent Zn^{2+} probes.[1i,3a] The importance of substitution at the pyrrolic α- and β'-carbons has been well elucidated, and these results offer a good strategy for the development of relevant Zn^{2+} probes. On the other hand, the meso substituents have also been demonstrated by us to have important effects on the oxidation and subsequent Zn^{2+} sensing behavior.[24e] More systematic work on the effects of the meso and the acyl substituents is now under way in our laboratory. In addition,

dx.doi.org/10.1021/jo400454e | J. Org. Chem. 2013, 78, 5328−5338

the unique α,β'-diacylated dipyrromethane **PS2** may be utilized for the synthesis of porphyrinoids, such as N-confused porphyrins.[25d]

EXPERIMENTAL SECTION

General Considerations. Commercially available solvents and reagents were used as received. Water was used after redistillation. UV−vis absorption and fluorescence spectra were recorded with a quartz cuvette (path length 1 cm). ^{1}H NMR and ^{13}C NMR spectra were measured on a 400 MHz spectrometer (^{1}H, 400 MHz; ^{13}C, 100 MHz) at 298 K with tetramethylsilane (TMS) as the internal standard. The electronic spray ionization (ESI) mass spectra were tested on a TOF mass spectrometer. 5-(Pentafluorophenyl)dipyrromethane was synthesized according to a reported procedure.[38]

UV/Vis Absorption Spectrum Measurements. The absorption spectra of **S1**−**S3** (10 μM) were measured at 25 °C in DMF and aqueous solution (DMF/50 mM HEPES, 4/1 v/v, pH 7.4). The tested ions Zn^{2+}, Na^+, K^+, Mg^{2+}, Ca^{2+}, Cd^{2+}, Hg^{2+}, Co^{2+}, Ni^{2+}, Cu^{2+}, and Pb^{2+} were added as acetate salts dissolved in DMF.

Fluorescence Emission Spectral Measurements. The fluorescence emission spectra of **S2** (10 μM) were measured at 25 °C in DMF and aqueous solution (DMF/50 mM HEPES, 4/1 v/v, pH 7.4), with excitation at λ 485 nm in DMF and 498 nm in HEPES buffer. The fluorescence spectra of **S1** and **S3** (10 μM) were measured in DMF with excitation at 462 nm for **S1** and 498 nm for **S3** (one of the isosbestic points). The slit width was 5 nm, and the PMT voltage was 600 V. The tested ions Zn^{2+}, Na^+, K^+, Mg^{2+}, Ca^{2+}, Cd^{2+}, Hg^{2+}, Co^{2+}, Ni^{2+}, Cu^{2+}, and Pb^{2+} were added as acetate salts dissolved in DMF.

Quantum Yield Measurements. The fluorescence quantum yields of **S1**−**S3** in DMF were measured using rhodamine 6G ($\Phi_{standard}$ = 0.94 in EtOH[31]) as a reference. The quantum yield Φ_{sample} was calculated using the equation[39]

$$\Phi_{sample} = \Phi_{standard} \times \left(\frac{F_{sample}}{F_{standard}}\right) \times \left(\frac{Abs_{standard}}{Abs_{sample}}\right) \times \left(\frac{n_{sample}}{n_{standard}}\right)^2$$

where Φ is the quantum yield, Abs is the absorbance of the solution at the excitation wavelength, F is the corrected emission intensity, and n is the average refractive index of the solution. The compounds were excited at the same wavelength (λ_{ex} 470 nm). The sample absorbance at the excitation wavelength was kept as low as possible (Abs_{ex} < 0.1). The slit width was 5 nm, and the PMT voltage was 550 V for both excitation and emission.

pH Influence Measurements. pH influence measurements were carried out in DMF mixed with the following buffers (4/1 v/v): MES buffer (50 mM, pH 5.7, 6.1 and 6.5), HEPES buffer (50 mM, pH 7.1 and 7.8), and CHES buffer (50 mM, pH 8.3, 8.7, 9.3 and 10.1). For pH 11.6, a mixture of CHES and NaOH was used as the buffer system.

Apparent Association Constant (K_{ass}) Measurements. The association constants were calculated on the basis of the titration of the probes **S1**−**S3** with Zn^{2+}. From Job plots, HRMS, and single-crystal structure diffraction analysis, we can conclude that the binding stoichiometry of probes **S1**−**S3** with Zn^{2+} is 2:1. Thus, the corresponding association constants were determined by a nonlinear least-squares fit of the titration data with the following equation for a 2:1 binding model:[32]

$$[Zn^{2+}] = \frac{x}{2K_{ass} \times (1-x)^2 \times [L]} + \frac{x \times [L]}{2}$$

where x is the fluorescence intensity ratio $(I - I_0)/(I_{max} - I_0)$ observed at the corresponding emission wavelength during addition of Zn^{2+}, $[Zn^{2+}]$ is the concentration of total added Zn^{2+}, K_{ass} is the association constant, and [L] is the concentration of the probe.

Crystallography. Single crystals suitable for X-ray analyses of **S2** and [Zn(**S1**)$_2$]·MeOH were obtained by slow evaporation of the MeOH/H_2O solutions of the corresponding compounds at room temperature. X-ray diffraction data were collected utilizing Mo Kα radiation (λ = 0.71073 Å). The structures were solved by direct methods and refined with full matrix least-squares techniques. Anisotropic thermal parameters were applied to all non-hydrogen atoms. All of the hydrogen atoms in these structures were located from differential electron density maps and constrained to ideal positions in the refinement procedure. All calculations were performed using the SHELX-97 software package.[40]

*Crystal data for **S2**:* $C_{31}H_{19}F_5N_2O_4$, M_w = 578.48, 0.31 × 0.21 × 0.18 mm^3, triclinic, $P\bar{1}$, a = 7.2931(9) Å, b = 13.1303(14) Å, c = 13.7726(15) Å, α = 92.7100(10)°, β = 96.3670(10)°, γ = 98.725(2)°, V = 1292.8(3) Å^3, F(000) = 592, ρ_{calcd} = 1.486 Mg m^{-3}, μ(Mo Kα) = 0.123 mm^{-1}, T = 298(2) K, 6822 data measured on a Bruker SMART Apex diffractometer, 4517 of which were unique (R_{int} = 0.0370), 381 parameters refined against F_o^2 (all data), final wR2 = 0.0964, S = 1.044, R1 ($I > 2\sigma(I)$) = 0.0528, largest final difference peak/hole +0.173/−0.208 e Å^{-3}, structure solution by direct methods and full-matrix least-squares refinement against F^2 (all data) using SHELXTL.

*Crystal data for [Zn(**S1**)$_2$]·MeOH:* $C_{47}H_{28}F_{10}N_4O_5Zn$, M_w = 984.10, 0.40 × 0.20 × 0.13 mm^3, triclinic, $P\bar{1}$, a = 12.8900(13) Å, b = 16.4959(15) Å, c = 21.712(2) Å, α = 92.2310(10)°, β = 90.2100(10)°, γ = 112.136(2)°, V = 4272.3(7) Å^3, F(000) = 1992, ρ_{calcd} = 1.530 Mg m^{-3}, μ(Mo Kα) = 0.672 mm^{-1}, T = 298(2) K, 21390 data measured on a Bruker SMART Apex diffractometer, 14733 of which were unique (R_{int} = 0.0661), 1213 parameters refined against F_o^2 (all data), final wR2 = 0.1576, S = 1.032, R1 ($I > 2\sigma(I)$) = 0.0732, largest final difference peak/hole +0.535/−0.629 e Å^{-3}, structure solution by direct methods and full-matrix least-squares refinement against F^2 (all data) using SHELXTL.

CCDC 914151 (**S2**) and 914152 ([Zn(**S1**)$_2$]·MeOH) contain the supplementary crystallographic data for this paper. These data can be obtained free of charge from The Cambridge Crystallographic Data Centre via www.ccdc.cam.ac.uk/data_request/cif.

DFT Calculations. All calculations were carried out using the Gaussian09 program package.[30] The geometries of all compounds were optimized by density functional calculations employing the hybrid B3LYP function. The LANL2DZ basis set was used for the Zn atom, while the 6-31G* basis set was adopted to describe other atoms. Subsequent single-point calculations were performed with the same method and basis sets but in a DMF solvent environment represented by the polarizable continuum model.

General Procedure for the Synthesis of Compounds PS1−PS3. Aluminum chloride (693 mg, 5.2 mmol) and *p*-anisoyl chloride (0.7 mL, 5.2 mmol) were added to a three-necked round-bottom flask, CH_2Cl_2 (50 mL) was added, and the solution was stirred at room temperature under N_2. After 3 h, a solution of 5-(pentafluorophenyl)-dipyrromethane (625 mg, 2.0 mmol) in 12.5 mL of CH_2Cl_2 was added dropwise at room temperature. After the mixture was stirred for another 2 h, water was added. The aqueous layer was extracted with CH_2Cl_2, and the combined extracts were washed with brine and dried over anhydrous Na_2SO_4. After removal of the solvent in vacuo, the crude product was separated by a silica gel column (eluted with 50/1 CH_2Cl_2/EA). **PS1** was obtained in 12% yield (107 mg), **PS2** was obtained in 48% yield (561 mg), and **PS3** was obtained in 21% yield (244 mg).

Improved Synthesis of PS1. Aluminum chloride (400 mg, 3 mmol) and *p*-anisoyl chloride (0.4 mL, 3 mmol) were added to a three-necked round-bottom flask, CH_2Cl_2 (50 mL) was added, and the solution was stirred at room temperature under N_2. After 3 h, a solution of 5-(pentafluorophenyl)dipyrromethane (625 mg, 2.0 mmol) in 12.5 mL of CH_2Cl_2 was added dropwise at room temperature. After the mixture was stirred for another 2 h, water was added. The aqueous layer was extracted with CH_2Cl_2, and the combined extracts were washed with brine and dried over anhydrous Na_2SO_4. After removal of the solvent in vacuo, the crude product was separated by a silica gel column (eluted with 50/1 CH_2Cl_2/EA). **PS1** was obtained in 45% yield (402 mg).

PS1. ^{1}H NMR ($CDCl_3$, 400 MHz, 298 K): δ 9.64 (s, 1H), 8.32 (s, 1H), 7.88 (d, J = 8.8 Hz, 2H), 6.97 (d, J = 8.8 Hz, 2H), 6.81−6.79 (br s, 1H), 6.77−6.76 (br s, 1H), 6.17 (t, 1H), 6.14 (s, 1H), 6.07 (t, 1H), 5.93 (s, 1H), 3.88 (s, 1H). ^{13}C NMR ($CDCl_3$, Bruker 100 MHz, 298 K): δ 183.6, 162.9, 136.7, 131.3, 131.1, 130.5, 126.6, 119.5, 118.7,

dx.doi.org/10.1021/jo400454e | J. Org. Chem. 2013, 78, 5328−5338

113.7, 110.0, 108.8, 108.4, 55.5. HRMS: obsd 447.1132, calcd for $C_{23}H_{16}N_2O_2F_5$ ([M + H]$^+$) 447.1132.

PS2. ^{1}H NMR ($CDCl_3$, 400 MHz, 298 K): δ 10.46 (s, 1H), 9.33 (s, 1H), 7.83 (d, J = 8.8 Hz, 2H), 7.78 (d, J = 8.7 Hz, 2H), 7.20−7.19 (br s, 1H), 6.95−6.91 (t, 4H), 6.75−6.74 (q, 1H), 6.52 (s, 1H), 6.08−6.07 (br s, 1H), 5.93 (s, 1H), 3.87 (s, 3H), 3.86 (s, 3H). ^{13}C NMR ($CDCl_3$, Bruker 100 MHz, 298 K): δ 189.6, 183.9, 163.1, 162.5, 136.4, 132.1, 131.4, 131.1, 130.2, 129.4, 125.8, 124.7, 120.1, 113.7, 113.4, 110.5, 109.4, 55.5, 55.4. HRMS: obsd 581.1498, calcd for $C_{31}H_{22}N_2O_4F_5$ ([M + H]$^+$) 581.1500.

PS3. ^{1}H NMR ($CDCl_3$, 400 MHz, 298 K): δ 10.98 (s, 2H), 7.82 (d, J = 8.4 Hz, 4H), 6.93 (d, J = 8.8 Hz, 4H), 6.63 (q, 2H), 6.12 (s, 1H), 6.07 (t, 2H), 3.86 (s, 6H). ^{13}C NMR ($CDCl_3$, Bruker 100 MHz, 298 K): δ 183.3, 162.8, 135.5, 131.7, 131.3, 130.6, 119.5, 113.4, 110.3, 55.4. HRMS: obsd 581.1497, calcd for $C_{31}H_{22}N_2O_4F_5$ ([M + H]$^+$) 581.1500.

Synthesis of S1. **PS1** (446 mg, 1 mmol) was dissolved in 250 mL of CH_2Cl_2, then DDQ (454 mg, 2 mmol) was added. The mixture was stirred at room temperature for 1 h and then directly purified by a silica gel column (eluent CH_2Cl_2) to afford the crude product **S1**, which was recrystallized from CH_2Cl_2 and *n*-hexane to afford a brown solid (271 mg, yield 61%). ^{1}H NMR ($CDCl_3$, 400 MHz, 298 K): δ 12.86 (s, 1H), 8.15 (s, 1H), 7.98 (d, J = 8.8 Hz, 2H), 7.00 (d, J = 8.8 Hz, 2H), 6.81 (d, J = 4.4 Hz, 1H), 6.70 (d, J = 4.8 Hz, 1H), 6.64 (d, J = 4.8 Hz, 1H), 6.27 (d, J = 4.4 Hz, 1H), 3.90 (s, 3H). ^{13}C NMR ($CDCl_3$, Bruker 100 MHz, 298 K): δ 183.9, 163.2, 162.6, 152.1, 139.3, 135.1, 133.2, 131.5, 130.5, 127.7, 122.5, 119.9, 118.8, 113.8, 55.5. HRMS: obsd 445.0975, calcd for $C_{23}H_{14}N_2O_2F_5$ ([M + H]$^+$) 445.0975.

Synthesis of S2. **PS2** (580.5 mg, 1 mmol) was dissolved in 250 mL of CH_2Cl_2, and then DDQ (454 mg, 2 mmol) was added. The mixture was stirred at room temperature for 24 h and then directly purified by a silica gel column (eluent CH_2Cl_2/MeOH 100/1) to afford the crude product **S2**, which was recrystallized from CH_2Cl_2 and *n*-hexane to afford a red solid (396 mg, yield: 69%). ^{1}H NMR ($CDCl_3$, 400 MHz, 298 K): δ 12.85 (s, 1H), 8.29 (d, J = 0.84 Hz, 1H), 8.07 (d, J = 8.8 Hz, 2H), 7.83 (d, J = 8.8 Hz, 2H), 7.03−7.01 (m, 3H), 6.98 (d, J = 1.8 Hz, 2H), 6.93 (d, J = 4.3 Hz, 1H), 6.52 (d, J = 4.3 Hz, 1H), 3.92 (s, 3H), 3.89 (s, 3H). ^{13}C NMR ($CDCl_3$, Bruker 100 MHz, 298 K): δ 188.3, 184.9, 163.7, 163.4, 154.4, 147.9, 146.1, 139.6, 135.8, 132.8, 131.9, 131.3, 130.9, 129.9, 127.3, 125.3, 121.3, 113.9, 55.6, 55.5. HRMS: obsd 579.1343, calcd for $C_{31}H_{20}N_2O_4F_5$ ([M + H]$^+$) 579.1343.

Synthesis of S3. **PS3** (299 mg, 0.52 mmol) was dissolved in 175 mL of CH_2Cl_2, and then DDQ (945 mg, 4.2 mmol) was added. The mixture was stirred at room temperature for 36 h and then directly purified by a silica gel column (eluent CH_2Cl_2/MeOH 100/1) to afford the crude product **S3**, which was recrystallized from CH_2Cl_2 and *n*-hexane to afford a red solid (290 mg, yield: 97%). ^{1}H NMR ($CDCl_3$, 400 MHz, 298 K): δ 12.62 (s, 1H), 8.21 (d, J = 8.9 Hz, 4H), 7.06 (d, J = 4.4 Hz, 2H), 7.03 (d, J = 8.9 Hz, 4H), 6.60 (d, J = 4.4 Hz, 2H), 3.91 (s, 6H). ^{13}C NMR ($CDCl_3$, Bruker 100 MHz, 298 K): δ 185.1, 163.7, 153.9, 143.6, 132.2, 129.5, 127.7, 126.7, 123.7, 114.0, 55.5. HRMS: obsd 579.1336, calcd for $C_{31}H_{20}N_2O_4F_5$ ([M + H]$^+$) 579.1343.

Synthesis of Zn(S1)$_2$. A mixture of **S1** (44 mg, 0.1 mmol) and $Zn(OAc)_2{\cdot}2H_2O$ (22 mg, 0.1 mmol) was dissolved in 50 mL of MeOH. The mixture was stirred at room temperature for 30 min and then directly purified by a silica gel column to afford the crude product Zn(**S1**)$_2$, which was recrystallized from CH_2Cl_2 and *n*-hexane to afford a dark green solid (39 mg, yield 83%). UV−vis (DMF) λ_{max} (nm): 519. ^{1}H NMR ($CDCl_3$, 400 MHz, 298 K): δ 7.92 (d, J = 8.88 Hz, 4H), 7.28 (s, 2H), 6.95 (d, J = 4.04 Hz, 2H), 6.90 (d, J = 8.84 Hz, 4H), 6.67 (d, J = 4.48 Hz, 2H), 6.55 (d, J = 4.0 Hz, 2H), 6.39 (q, 2H), 3.84 (s, 6H). ^{13}C NMR ($CDCl_3$, 100 MHz, 298 K): δ 185.9, 162.4, 158.4, 147.8, 145.29, 145.27, 145.2, 143.3, 140.2, 133.8, 131.2, 130.2, 129.7, 125.4, 123.1, 119.3, 112.9, 54.9, 52.9. IR (KBr pellet, cm^{-1}): 3359 (w), 2923 (s), 2852 (m), 1658 (m), 1632 (m), 1596 (m), 1569 (m), 1521 (m), 1500 (m), 1455 (m), 1411 (m), 1366 (w), 1321 (s), 1306 (s), 1252 (s), 1169 (s), 1083 (w), 1019 (s), 989 (s), 941 (m), 875 (w), 840 (m), 752 (m), 640 (w), 619 (w). HRMS: obsd 951.1003, calcd for $C_{46}H_{25}N_4O_4F_{10}Zn$ ([M + H]$^+$) 951.1008.

Synthesis of Zn(S2)$_2$. This complex was synthesized as a deep red solid (49 mg, yield 80%) by a procedure similar to that for Zn(**S1**)$_2$. UV−vis (DMF) λ_{max} (nm): 544. ^{1}H NMR ($CDCl_3$, 400 MHz, 298 K): δ 7.92 (d, J = 8.88 Hz, 4H), 7.71 (t, 4H), 7.68 (s, 2H), 7.09 (s, 2H), 7.00 (d, J = 4.2 Hz, 2H), 6.92 (d, J = 8.88 Hz, 4H), 6.88 (d, J = 8.84 Hz, 4H), 6.75 (d, J = 4.2 Hz, 2H), 3.85 (s, 6H), 3.84 (s, 6H). ^{13}C NMR ($CDCl_3$, 100 MHz, 298 K): δ 187.7, 185.9, 162.9, 162.6, 156.0, 151.4, 143.6, 141.2, 135.8, 134.3, 134.1, 131.4, 130.8, 129.5, 129.4, 120.6, 113.24, 113.16, 54.96, 54.91. IR (KBr pellet, cm^{-1}): 3357 (w), 2917 (m), 2847 (m), 1635 (w), 1599 (m), 1552 (m), 1494 (w), 1453 (w), 1424 (m), 1300 (s), 1281 (s), 1249 (s), 1167 (s), 1067 (w), 1021 (m), 994 (s), 955 (s), 878 (s), 851 (m), 793 (w), 744 (m), 648 (w), 619 (w). HRMS: obsd 1219.1744, calcd for $C_{62}H_{37}N_4O_8F_{10}Zn$ ([M + H]$^+$) 1219.1743.

Synthesis of Zn(S3)$_2$. This complex was synthesized as a deep red solid (44 mg, yield 72%) by a procedure similar to that for Zn(**S1**)$_2$. UV−vis (DMF) λ_{max} (nm): 535. ^{1}H NMR ($CDCl_3$, 400 MHz, 298 K): δ 7.69 (d, J = 8.84 Hz, 8H), 6.71 (d, J = 8.84 Hz, 8H), 6.54 (t, 8H), 3.76 (s, 12H). ^{13}C NMR ($CDCl_3$, 100 MHz, 298 K): δ 186.5, 184.6, 163.2, 162.7, 156.2, 153.5, 143.2, 143.1, 142.4, 131.7, 131.4, 130.6, 129.5, 129.1, 127.1, 123.1, 121.1, 113.5, 112.7, 54.9, 54.8, 29.2. IR (KBr pellet, cm^{-1}): 3361 (w), 2921 (m), 2851 (w), 1652 (m), 1600 (s), 1561 (m), 1500 (m), 1415 (w), 1341 (w), 1250 (s), 1165 (s), 1065 (m), 992 (s), 943 (m), 889 (w), 845 (s), 748 (m), 644 (w), 615 (w). HRMS: obsd 1219.1747, calcd for $C_{62}H_{37}N_4O_8F_{10}Zn$ ([M + H]$^+$) 1219.1743.

■ ASSOCIATED CONTENT

Supporting Information

Figures, tables, and CIF files giving the ^{1}H/^{13}C NMR and HRMS spectra of compounds **PS1**−**PS3** and **S1**−**S3**, calculated structures of **S1** and **S2**, UV−vis and fluorescence spectra, Job plots, apparent association constant (K_{ass}) determination, and detection limits of **S1**−**S3**, ^{1}H NMR and HRMS spectra of complexes Zn(**S1**)$_2$, **Zn(S2$_2$)** and Zn(**S3**)$_2$, full crystal data of **S2** and Zn(**S1**)$_2$·MeOH containing complete details of data collection, crystal and unit-cell parameters, structure solution and refinement, and tables of atomic coordinates and bond lengths, and calculated absolute energy levels of **S1**−**S3** and their corresponding zinc complexes. This material is available free of charge via the Internet at http://pubs.acs.org.

■ AUTHOR INFORMATION

Corresponding Author

*E-mail for Y.X.: yshxie@ecust.edu.cn.

Notes

The authors declare no competing financial interest.

■ ACKNOWLEDGMENTS

This work was financially supported by the NSFC (21072060), the Program for Professor of Special Appointment (Eastern Scholar) at Shanghai Institutions of Higher Learning, Program for New Century Excellent Talents in University (NCET), the Innovation Program of Shanghai Municipal Education Commission, the Fundamental Research Funds for the Central Universities (WK1013002), and the SRFDP (20100074110015).

■ REFERENCES

(1) (a) Beer, P. D.; Gale, P. A. *Angew. Chem., Int. Ed.* **2001**, *40*, 486−516. (b) Hanaoka, K.; Kikuchi, K.; Kojima, H.; Urano, Y.; Nagano, T. *Angew. Chem., Int. Ed.* **2003**, *42*, 2996−2999. (c) Gai, L.; Chen, H.; Zou, B.; Lu, H.; Lai, G.; Li, Z.; Shen, Z. *Chem. Commun.* **2012**, *48*,

10721−10723. (d) Hill, J. P.; Subbaiyan, N. K.; D'Souza, F.; Xie, Y.; Sahu, S.; Sanchez-Ballester, N. M.; Richards, G. J.; Mori, T.; Ariga, K. *Chem. Commun.* **2012**, *48*, 3951−3953. (e) Cheng, X.; Li, S.; Jia, H.; Zhong, A.; Zhong, C.; Feng, J.; Qin, J.; Li, Z. *Chem. Eur. J.* **2012**, *18*, 1691−1699. (f) Plitt, P.; Gross, D. E.; Lynch, V. M.; Sessler, J. L. *Chem. Eur. J.* **2007**, *13*, 1374−1381. (g) Que, E. L.; Domaille, D. W.; Chang, C. J. *Chem. Rev.* **2008**, *108*, 1517−1549. (h) Galbraith, E.; James, T. D. *Chem. Soc. Rev.* **2010**, *39*, 3831−3842. (i) Xu, Z. C.; Yoon, J.; Spring, D. R. *Chem. Soc. Rev.* **2010**, *39*, 1996−2006. (j) Qian, F.; Zhang, C.; Zhang, Y.; He, W.; Gao, X.; Hu, P.; Guo, Z. *J. Am. Chem. Soc.* **2009**, *131*, 1460−1468. (k) Yuan, L.; Lin, W.; Zhao, S.; Gao, W.; Chen, B.; He, L.; Zhu, S. *J. Am. Chem. Soc.* **2012**, *134*, 13510−13523. (l) Li, A. F.; He, H.; Ruan, Y. B.; Wen, Z. C.; Zhao, J. S.; Jiang, Q. J.; Jiang, Y. B. *Org. Biomol. Chem.* **2009**, *7*, 193−200. (m) Peng, L. H.; Wang, M.; Zhang, G. X.; Zhang, D. Q.; Zhu, D. B. *Org. Lett.* **2009**, *11*, 1943−1946. (n) Xue, L.; Liu, Q.; Jiang, H. *Org. Lett.* **2009**, *11*, 3454−3457.

(2) (a) Tomat, E.; Lippard, S. J. *Curr. Opin. Chem. Biol.* **2010**, *14*, 225−230. (b) Frederickson, C. J.; Koh, J. Y.; Bush, A. I. *Nat. Rev. Neurosci.* **2005**, *6*, 449−462. (c) Vallee, B. L.; Falchuk, K. H. *Anglais* **1993**, *73*, 79−118.

(3) (a) Jiang, P.; Guo, Z. *Coord. Chem. Rev.* **2004**, *248*, 205−229. (b) Lin, W.; Feng, J.; Yuan, L.; Tan, W. *Sens. Actuators, B* **2009**, *135*, 512−515.

(4) (a) Chang, C. J.; Nolan, E. M.; Jaworski, J.; Burdette, S. C.; Sheng, M.; Lippard, S. J. *Chem. Biol.* **2004**, *11*, 203−210. (b) Nolan, E. M.; Ryu, J. W.; Jaworski, J.; Feazell, R. P.; Sheng, M.; Lippard, S. J. *J. Am. Chem. Soc.* **2006**, *128*, 15517−15528.

(5) Lee, A. E.; Grace, M. R.; Meyer, A. G.; Tuck, K. L. *Tetrahedron Lett.* **2010**, *51*, 1161−1165.

(6) (a) Xu, Z. C.; Baek, K. H.; Kim, H. N.; Cui, J. N.; Qian, X. H.; Spring, D. R.; Shin, I.; Yoon, J. *J. Am. Chem. Soc.* **2010**, *132*, 601−610. (b) Lu, C.; Xu, Z.; Cui, J.; Zhang, R.; Qian, X. *J. Org. Chem.* **2007**, *72*, 3554−3557.

(7) (a) Lim, N. C.; Schuster, J. V.; Porto, M. C.; Tanudra, M. A.; Yao, L.; Freake, H. C.; Brückner, C. *Inorg. Chem.* **2005**, *44*, 2018−2030. (b) Mizukami, S.; Okada, S.; Kimura, S.; Kikuchi, K. *Inorg. Chem.* **2009**, *48*, 7630−7638.

(8) (a) Mikata, Y.; Ugai, A.; Yasuda, K.; Itami, S.; Tamotsu, S.; Konno, H.; Iwatsuki, S. *Chem. Biodivers.* **2012**, *9*, 2064−2075. (b) Xue, L.; Wang, H. H.; Wang, X. J.; Jiang, H. *Inorg. Chem.* **2008**, *47*, 4310−4318. (c) Du, J. J.; Fan, J. L.; Peng, X. J.; Li, H. L.; Sun, S. G. *Sens. Actuators, B* **2010**, *144*, 337−341.

(9) (a) Tang, B.; Huang, H.; Xu, K.; Tong, L.; Yang, G.; Liu, X.; An, L. *Chem. Commun.* **2006**, 3609−3611. (b) Kiyose, K.; Kojima, H.; Urano, Y.; Nagano, T. *J. Am. Chem. Soc.* **2006**, *128*, 6548−6549.

(10) (a) Han, Z.; Zhang, X.; Li, Z.; Gong, Y.; Wu, X.; Jin, Z.; He, C.; Jian, L.; Zhang, J.; Shen, G.; Yu, R. *Anal. Chem.* **2010**, *82*, 3108−3113. (b) Sasaki, H.; Hanaoka, K.; Urano, Y.; Terai, T.; Nagano, T. *Bioorg. Med. Chem.* **2011**, *19*, 1072−1078.

(11) (a) Wu, Y. K.; Peng, X. J.; Guo, B. C.; Fan, J. L.; Zhang, Z. C.; Wang, J. Y.; Cui, A. J.; Gao, Y. L. *Org. Biomol. Chem.* **2005**, *3*, 1387−1392. (b) Atilgan, S.; Ozdemir, T.; Akkaya, E. U. *Org. Lett.* **2008**, *10*, 4065−4067.

(12) (a) Jiang, W.; Fu, Q.; Fan, H.; Wang, W. *Chem. Commun.* **2008**, 259−261. (b) Wong, B. A.; Friedle, S.; Lippard, S. J. *J. Am. Chem. Soc.* **2009**, *131*, 7142−7152.

(13) (a) Liu, Z.; Zhang, C.; Chen, Y.; He, W.; Guo, Z. *Chem. Commun.* **2012**, *48*, 8365−8367. (b) Xue, L.; Liu, C.; Jiang, H. *Org. Lett.* **2009**, *11*, 1655−1658.

(14) (a) Vinkenborg, J. L.; Nicolson, T. J.; Bellomo, E. A.; Koay, M. S.; Rutter, G. A.; Merkx, M. *Nat. Meth.* **2009**, *6*, 737−740. (b) Zhu, J. F.; Yuan, H.; Chan, W. H.; Lee, A. W. M. *Tetrahedron Lett.* **2010**, *51*, 3550−3554.

(15) Manandhar, E.; Broome, J. H.; Myrick, J.; Lagrone, W.; Cragg, P. J.; Wallace, K. J. *Chem. Commun.* **2011**, *47*, 8796−8798.

(16) (a) Hong, Y.; Chen, S.; Leung, C. W. T.; Lam, J. W. Y.; Liu, J.; Tseng, N. W.; Kwok, R. T. K.; Yu, Y.; Wang, Z.; Tang, B. Z. *ACS Appl. Mater. Interfaces* **2011**, *3*, 3411−3418. (b) Sun, F.; Zhang, G.; Zhang, D.; Xue, L.; Jiang, H. *Org. Lett.* **2011**, *13*, 6378−6381.

(17) (a) Zhang, B.; Cao, K. S.; Xu, Z. A.; Yang, Z. Q.; Chen, H. W.; Huang, W.; Yin, G.; You, X. Z. *Eur. J. Inorg. Chem.* **2012**, *2012*, 3844−3851. (b) Huston, M. E.; Haider, K. W.; Czarnik, A. W. *J. Am. Chem. Soc.* **1988**, *110*, 4460−4462. (c) Zhou, Y.; Li, Z. X.; Zang, S. Q.; Zhu, Y. Y.; Zhang, H. Y.; Hou, H. W.; Mak, T. C. W. *Org. Lett.* **2012**, *14*, 1214−1217.

(18) (a) Ambrosi, G.; Formica, M.; Fusi, V.; Giorgi, L.; Macedi, E.; Micheloni, M.; Paoli, P.; Pontellini, R.; Rossi, P. *Inorg. Chem.* **2010**, *49*, 9940−9948. (b) El Majzoub, A.; Cadiou, C.; Déchamps Olivier, I.; Tinant, B.; Chuburu, F. *Inorg. Chem.* **2011**, *50*, 4029−4038.

(19) (a) Bruckner, C.; Karunaratne, V.; Rettig, S. J.; Dolphin, D. *Can. J. Chem.* **1996**, *74*, 2182−2193. (b) Miao, Q.; Shin, J. Y.; Patrick, B. O.; Dolphin, D. *Chem. Commun.* **2009**, 2541−2543. (c) Wood, T. E.; Thompson, A. *Chem. Rev.* **2007**, *107*, 1831−1861.

(20) (a) Ikeda, C.; Ueda, S.; Nabeshima, T. *Chem. Commun.* **2009**, 2544−2546. (b) Sutton, J. M.; Rogerson, E.; Wilson, C. J.; Sparke, A. E.; Archibald, S. J.; Boyle, R. W. *Chem. Commun.* **2004**, 1328−1329. (c) Hanson, K.; Tamayo, A.; Diev, V. V.; Whited, M. T.; Djurovich, P. I.; Thompson, M. E. *Inorg. Chem.* **2010**, *49*, 6077−6084. (d) McLean, T. M.; Moody, J. L.; Waterland, M. R.; Telfer, S. G. *Inorg. Chem.* **2011**, *51*, 446−455. (e) Teets, T. S.; Partyka, D. V.; Esswein, A. J.; Updegraff, J. B.; Zeller, M.; Hunter, A. D.; Gray, T. G. *Inorg. Chem.* **2007**, *46*, 6218−6220. (f) Thoi, V. S.; Stork, J. R.; Magde, D.; Cohen, S. M. *Inorg. Chem.* **2006**, *45*, 10688−10697. (g) Halper, S. R.; Do, L.; Stork, J. R.; Cohen, S. M. *J. Am. Chem. Soc.* **2006**, *128*, 15255−15268. (h) Kobayashi, J.; Kushida, T.; Kawashima, T. *J. Am. Chem. Soc.* **2009**, *131*, 10836−10837. (i) Maeda, H.; Hasegawa, M.; Hashimoto, T.; Kakimoto, T.; Nishio, S.; Nakanishi, T. *J. Am. Chem. Soc.* **2006**, *128*, 10024−10025. (j) Sakamoto, N.; Ikeda, C.; Yamamura, M.; Nabeshima, T. *J. Am. Chem. Soc.* **2011**, *133*, 4726−4729. (k) Sazanovich, I. V.; Kirmaier, C.; Hindin, E.; Yu, L.; Bocian, D. F.; Lindsey, J. S.; Holten, D. *J. Am. Chem. Soc.* **2004**, *126*, 2664−2665. (l) Zhang, Y.; Thompson, A.; Rettig, S. J.; Dolphin, D. *J. Am. Chem. Soc.* **1998**, *120*, 13537−13538. (m) Hyun, A. R.; Kim, S. K.; Kang, I. N.; Park, J. W.; Shin, J. Y.; Song, O. K. *Mol. Cryst. Liq. Cryst.* **2007**, *463*, 33−39. (n) Crawford, S. M.; Ali, A. A. S.; Cameron, T. S.; Thompson, A. *Inorg. Chem.* **2011**, *50*, 8207−8213.

(21) Filatov, M. A.; Lebedev, A. Y.; Mukhin, S. N.; Vinogradov, S. A.; Cheprakov, A. V. *J. Am. Chem. Soc.* **2010**, *132*, 9552−9554.

(22) (a) Ulrich, G.; Ziessel, R.; Harriman, A. *Angew. Chem., Int. Ed.* **2008**, *47*, 1184−1201. (b) Loudet, A.; Burgess, K. *Chem. Rev.* **2007**, *107*, 4891−4932. (c) Boens, N.; Leen, V.; Dehaen, W. *Chem. Soc. Rev.* **2012**, *41*, 1130−1172.

(23) Ding, Y. B.; Xie, Y. S.; Li, X.; Hill, J. P.; Zhang, W. B.; Zhu, W. H. *Chem. Commun.* **2011**, *47*, 5431−5433.

(24) (a) Xie, Y. S.; Morimoto, T.; Furuta, H. *Angew. Chem., Int. Ed.* **2006**, *45*, 6907−6910. (b) Wang, Q. G.; Xie, Y. S.; Ding, Y. B.; Li, X.; Zhu, W. H. *Chem. Commun.* **2010**, *46*, 3669−3671. (c) Lu, X.; Zhu, W.; Xie, Y.; Li, X.; Gao, Y.; Li, F.; Tian, H. *Chem. Eur. J.* **2010**, *16*, 8355−8364. (d) Ding, Y. B.; Li, T.; Zhu, W. H.; Xie, Y. S. *Org. Biomol. Chem.* **2012**, *10*, 4201−4207. (e) Ding, Y.; Li, T.; Li, X.; Zhu, W.; Xie, Y. *Org. Biomol. Chem.* **2013**, *11*, 2685−2692. (f) Xie, Y. S.; Ding, Y. B.; Li, X.; Wang, C.; Hill, J. P.; Ariga, K.; Zhang, W. B.; Zhu, W. H. *Chem. Commun.* **2012**, *48*, 11513−11515.

(25) (a) Anand, V. G.; Saito, S.; Shimizu, S.; Osuka, A. *Angew. Chem., Int. Ed.* **2005**, *44*, 7244−7248. (b) Toganoh, M.; Furuta, H. *Chem. Commun.* **2012**, *48*, 937−954. (c) Li, W. S.; Jiang, D. L.; Suna, Y.; Aida, T. *J. Am. Chem. Soc.* **2005**, *127*, 7700−7702. (d) Maeda, H.; Morimoto, T.; Osuka, A.; Furuta, H. *Chem. Asian. J.* **2006**, *1*, 832−844.

(26) (a) Kim, E.; Park, S. B. *Chem. Asian J.* **2009**, *4*, 1646−1658. (b) Amendola, V.; Fabbrizzi, L.; Foti, F.; Licchelli, M.; Mangano, C.; Pallavicini, P.; Poggi, A.; Sacchi, D.; Taglietti, A. *Coord. Chem. Rev.* **2006**, *250*, 273−299. (c) Dickinson, B. C.; Huynh, C.; Chang, C. J. *J. Am. Chem. Soc.* **2010**, *132*, 5906−5915. (d) Kim, E.; Koh, M.; Lim, B. J.; Park, S. B. *J. Am. Chem. Soc.* **2011**, *133*, 6642−6649. (e) Liu, Q.; Yang, T. S.; Feng, W.; Li, F. Y. *J. Am. Chem. Soc.* **2012**, *134*, 5390−5397.

(27) (a) Gokulnath, S.; Yamaguchi, K.; Toganoh, M.; Mori, S.; Uno, H.; Furuta, H. *Angew. Chem., Int. Ed.* **2011**, *50*, 2302−2306. (b) Gupta, I.; Srinivasan, A.; Morimoto, T.; Toganoh, M.; Furuta, H. *Angew. Chem., Int. Ed.* **2008**, *47*, 4563−4567. (c) Xie, Y. S.; Yamaguchi, K.; Toganoh, M.; Uno, H.; Suzuki, M.; Mori, S.; Saito, S.; Suka, A.; Furuta, H. *Angew. Chem., Int. Ed.* **2009**, *48*, 5496−5499.
(28) (a) Tsuchimoto, T. *Chem. Eur. J.* **2011**, *17*, 4064−4075. (b) Cadamuro, S.; Degani, I.; Dughera, S.; Fochi, R.; Gatti, A.; Piscopo, L. *J. Chem. Soc., Perkin Trans. 1* **1993**, 273−283.
(29) (a) Rao, P. D.; Dhanalekshmi, S.; Littler, B. J.; Lindsey, J. S. *J. Org. Chem.* **2000**, *65*, 7323−7344. (b) Tamaru, S.; Yu, L. H.; Youngblood, W. J.; Muthukumaran, K.; Taniguchi, M.; Lindsey, J. S. *J. Org. Chem.* **2004**, *69*, 765−777.
(30) (a) Tomasi, J.; Mennucci, B.; Cammi, R. *Chem. Rev.* **2005**, *105*, 2999−3093. (b) Frisch, M. J.; Trucks, G. W.; Schlegel, H. B.; Scuseria, G. E.; Robb, M. A.; Cheeseman, J. R.; Scalmani, G.; Barone, V.; Mennucci, B.; Petersson, G. A.; et al. *Gaussian 09, Revision A.2*; Gaussian, Inc., Wallingford, CT, 2009. (c) Becke, A. D. *J. Chem. Phys.* **1993**, *98*, 5648−5652. (d) Hehre, W. J.; Ditchfield, R.; Pople, J. A. *J. Chem. Phys.* **1972**, *56*, 2257−2261.
(31) Fischer, M.; Georges, J. *Chem. Phys. Lett.* **1996**, *260*, 115−118.
(32) (a) Bourson, J.; Pouget, J.; Valeur, B. *J. Phys. Chem.* **1993**, *97*, 4552−4557. (b) Yang, M. H.; Thirupathi, P.; Lee, K. H. *Org. Lett.* **2011**, *13*, 5028−5031. (c) Kubo, Y.; Kato, M.; Misawa, Y.; Tokita, S. *Tetrahedron Lett.* **2004**, *45*, 3769−3773.
(33) Shortreed, M.; Kopelman, R.; Kuhn, M.; Hoyland, B. *Anal. Chem.* **1996**, *68*, 1414−1418.
(34) Weiss, J. H.; Sensi, S. L.; Koh, J. Y. *Trends Pharmacol. Sci.* **2000**, *21*, 395−401.
(35) Lim, N. C.; Bruckner, C. *Chem. Commun.* **2004**, 1094−1095.
(36) (a) Liu, Y. L.; Ai, K. L.; Cheng, X. L.; Huo, L. H.; Lu, L. H. *Adv. Funct. Mater.* **2010**, *20*, 951−956. (b) Shang, L.; Zhang, L.; Dong, S. *Analyst* **2009**, *134*, 107−113. (c) Bao, Y.; Liu, B.; Wang, H.; Tian, J.; Bai, R. *Chem. Commun.* **2011**, *47*, 3957−3959. (d) Jo, J.; Lee, H. Y.; Liu, W.; Olasz, A.; Chen, C. H.; Lee, D. *J. Am. Chem. Soc.* **2012**, *134*, 16000−16007. (e) Sokkalingam, P.; Lee, C. H. *J. Org. Chem.* **2011**, *76*, 3820−3828. (f) Jung, H. S.; Han, J. H.; Kim, Z. H.; Kang, C.; Kim, J. S. *Org. Lett.* **2011**, *13*, 5056−5059. (g) Sun, Y.; Liu, Y. L.; Chen, M. L.; Guo, W. *Talanta* **2009**, *80*, 996−1000. (h) Sumiya, S.; Doi, T.; Shiraishi, Y.; Hirai, T. *Tetrahedron* **2012**, *68*, 690−696. (i) Zang, L.; Wei, D.; Wang, S.; Jiang, S. *Tetrahedron* **2012**, *68*, 636−641.
(37) (a) Ikawa, Y.; Takeda, M.; Suzuki, M.; Osuka, A.; Furuta, H. *Chem. Commun.* **2010**, *46*, 5689−5691. (b) Hung, C. H.; Chang, G. F.; Kumar, A.; Lin, G. F.; Luo, L. Y.; Ching, W. M.; Diau, E. W. G. *Chem. Commun.* **2008**, 978−980.
(38) Littler, B. J.; Miller, M. A.; Hung, C. H.; Wagner, R. W.; O'Shea, D. F.; Boyle, P. D.; Lindsey, J. S. *J. Org. Chem.* **1999**, *64*, 1391−1396.
(39) Eaton, D. F. *Pure Appl. Chem.* **1988**, *60*, 1107−1114.
(40) Sheldrick, G. M. *Acta Crystallogr., Sect. A* **2008**, *64*, 112.